

Y. Zu, C.-H. Chan, S.-W. Sin, S.-P. U, R.P. Martins, F. Maloberti: "**A 35 fJ 10b 160 MS/s Pipelined-SAR ADC with Decoupled Flip-Around MDAC and Self-Embedded Offset Cancellation**"; IEEE Asian Solid-State Circuits Conference, A-SSCC 2011, Jeju, 14-16 November 2011, pp. 61-64.

©20xx IEEE. Personal use of this material is permitted. However, permission to reprint/republish this material for advertising or promotional purposes or for creating new collective works for resale or redistribution to servers or lists, or to reuse any copyrighted component of this work in other works must be obtained from the IEEE.

# A 35 fJ 10b 160 MS/s Pipelined-SAR ADC with Decoupled Flip-Around MDAC and Self-Embedded Offset Cancellation

Yan Zhu, Chi-Hang Chan, Sai-Weng Sin, Seng-Pan U, R.P.Martins<sup>1</sup>, Franco Maloberti<sup>2</sup>

State-Key Laboratory of Analog and Mixed Signal VLSI ([http://www.fst.umac.mo/en/lab/ans\\_vlsi/index.html](http://www.fst.umac.mo/en/lab/ans_vlsi/index.html))

Faculty of Science and Technology, University of Macau, Macao, China

E-mail: [yanjulia@ieee.org](mailto:yanjulia@ieee.org)

1 - On leave from Instituto Superior Técnico/TU of Lisbon, Portugal

2 - University of Pavia, Italy

**Abstract** - A Time-Interleaved (TI) pipelined-SAR ADC with on-chip offset cancellation technique is presented. The design reuses the SAR ADC to perform offset cancellation, which significantly saves calibration area, power and time. A 6 bit capacitive DAC is built as a flip-around MDAC for low inter-stage gain implementation. The capacitive attenuation solutions in both 1<sup>st</sup> and 2<sup>nd</sup> DACs minimize the power dissipation and optimize conversion speed. Measurements of a 65nm CMOS prototype operating at 160MS/s and 1.1V supply show 2.72mW total power consumption. The SNDR is 55.4dB and the FoM as low as 35fJ/conv.-step.

## I. INTRODUCTION

This paper confirms the excellent power effectiveness of the time-interleaved (TI) pipeline-SAR ADC architecture. Compared to the results published in [1], the use of an effective calibration method and full capacitive DACs (CDACs) reduces the FoM by 40% with a 2.6 times increase in conversion speed. The technique overcomes the speed bottleneck of SAR ADCs and achieves competitive lower power dissipation when compared with pipelined ADCs. The three key limitations caused by comparator offset; the unavailable of low power flip-around MDAC; the requirements of static power for the reference voltage generator are properly resolved.

For less than 6b offset correction with an analog method, like a ring-counter-based offset calibration [2], or with a digital method like the background averaging [1] is relatively simple and accurate. However, for medium resolution of 8-10b the calibration usually requires on-chip complex logic algorithms that consumes large area and power. Thus, for securing low power it is necessary to use methods that explore analog and digital features to minimize hardware and attain flexibility.

The pipelined-SAR architecture uses the 1<sup>st</sup> stage CDAC to perform the residue amplification. However, the capacitive ratio of residue amplification is heavily linked with the resolution of 1<sup>st</sup> stage SAR DAC array. To achieve a high-resolution SAR conversion in front-end CDAC, the flip-around MDAC is difficult

This research work was financially supported by Research Grants of University of Macau and Macao Science & Technology Development Fund (FDCT).

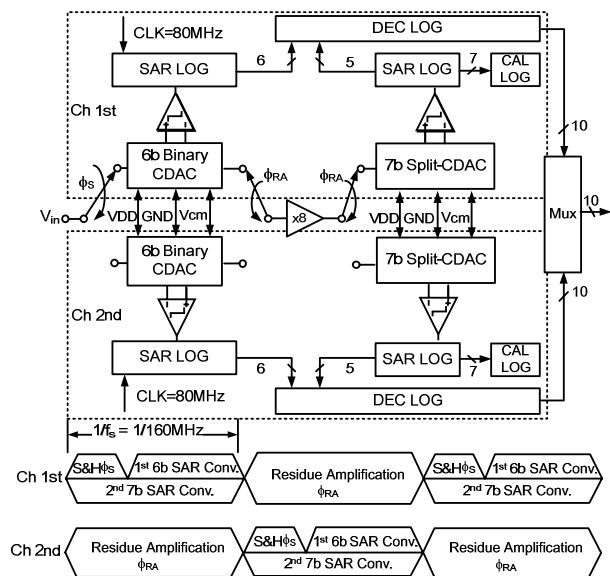


Fig. 1: Overall ADC architecture and its timing diagram.

to be implemented [3]. Previous works either adopted power hungry resistive ladder that helps the limited resolution in capacitive DAC to enable the flip-around MDAC [1], or an additional resetting capacitor is required for a non-flip-around amplification with reduced feedback factor [3]-[5].

The time-interleaved (TI) pipeline-SAR ADC of this paper corrects the offset with a self-embedded foreground calibration scheme by reusing the 2<sup>nd</sup>-stage SAR ADC. The calibration range of the offset can go up to full-scale reference of the 2<sup>nd</sup> stage with the request of very small area and digital power. The 1<sup>st</sup> stage CDAC array utilized the partial feedback capacitor that allow decoupling the DAC array resolution and the residue gain ratio, thus enabling power efficient flip-around MDAC implementation. The CDACs in 1<sup>st</sup> and 2<sup>nd</sup> stage SAR ADCs are proper designed to perform both 8xresidue amplification and reference-buffer-free SA conversion. The experimental results of the 65 nm CMOS prototype verify the effectiveness of the method with state-of-the

art results for medium resolution and conversion speed in the 100-200 MS/s range.

## II. ADC ARCHITECTURE

Fig. 1 shows the ADC architecture and timing diagram. The scheme is composed by two interleaved pipelined-SAR ADCs with a residue amplifier shared by the two channels (similar to [1]). Each channel uses 6b and 7b SAR ADCs (2b of the second stage are for offset cancellation) with 1 bit overlapping for digital error correction. The 1<sup>st</sup>-stage SAR converts the coarse 6b code and generates the residue at top-plate of the DAC, which is amplified by 8 to the 2<sup>nd</sup>-stage DAC. The 2<sup>nd</sup> SAR operates in a pipeline fashion while the first stage starts a new cycle. The 6b coarse and the 5b fine codes enter the digital correction logic to build the final 10b output. The two extra bit of the second stage used for offset calibration do not require extra time because the S&H phase is not necessary for 2<sup>nd</sup> SAR conversion. The gain mismatch between two TI channels determined by the inherit capacitor matching of 1<sup>st</sup>-stage CDAC is not problematic at 10b, while the inter-stage gain error caused by parasitic capacitance of DACs degrades the conversion linearity, which will be discussed in section IV.

## III. OFFSET-CANCELLATION

Time-interleaved architectures augment the conversion rate but suffer from the offset mismatches. These issues can be addressed with various solutions. Sharing the inter-stage amplifier avoids the offset mismatch in the residual generation. The use of digital error correction relaxes the conversion accuracy of the 1<sup>st</sup> SA decisions from 10b to 7b. Because of the relaxed matching accuracy the 1<sup>st</sup>-stage comparator offset is calibrated with the unbalanced capacitive loading method [6]. The residue amplification by 8 is a proper trade-off between power limits and accuracy. Since the required conversion accuracy in 2<sup>nd</sup>-stage is 8b with the offset requirement of 9b, it is necessary to use a more effective offset calibration method.

Fig. 2 shows block and timing diagrams of the 2<sup>nd</sup>-stage SAR ADC with the implementation of offset-cancellation technique. It is a 7b split DAC array used for both conventional SA conversion and offset measurement. In the calibration mode the input of the stage is set to zero. The output of the 2<sup>nd</sup>-stage DAC gives rise to the comparator offset with 9b accuracy. The value is stored on a memory to be subtracted afterwards during the normal SA

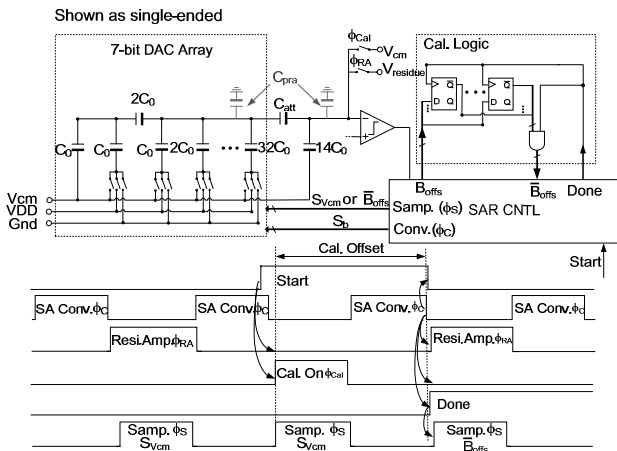


Fig. 2: 2<sup>nd</sup>-stage SAR ADC architecture and calibration timing diagram.

conversion. As Fig. 2 outlines when calibration is not active (Start=0), the residue is sampled at the top-plate of the DAC by connecting its bottom-plate to  $V_{cm}$  during the sampling ( $\Phi_S$ ). Since the input swing is relatively small ( $V_{p-p}=1/8V_{DD}$ ), the top-plate switch is sized smaller to avoid sampling nonlinearity due to the signal dependent charge injection of the switch. When calibration is active (Start=1), the residue amplification phase ( $\Phi_{RA}$ ) is disabled. Both top- and bottom-plates of the DAC are reset to  $V_{cm}$ . Since there is no initial charge in the capacitive array, two inputs of the comparator are set to zero. After 7b conversion ( $\Phi_C$ ) is completed (Done=1), the output of the DAC approximates to the comparator offset voltage according to switch control logic  $S_b$ , which are locked and stored by 7 flip-flops as offset code  $B_{offs}$ . When the next residue sampling phase  $\Phi_{RA}$  appears the offset cancellation is achieved by switching a 7b complementary offset code at DAC's bottom-plate instead of  $V_{cm}$ , consequently, leading to a value of  $V_{residue}-V_{offs}$  at the DAC's output for subsequent 5b SA comparison.

The technique allows the maximum offset cancellation range up to full-scale of the 2<sup>nd</sup>-stage reference voltage and compensates the offset with 1/4 LSB accuracy. The calibration logic, consisting of dynamic flip-flops and AND gates, are easily implemented with small area costs. The offset of the shared op-amp is not cancelled. However, a relatively low value is required as a large op-amp offset, other than causing an overall offset, limits the error tolerance range of the 1<sup>st</sup>-stage. This design obtains a  $3\sigma$  input referred op-amp's offset  $V_{off-opm}$  well within  $1/32 V_{FS-2nd}$  (The  $8xV_{off-opm}$  needs be suppressed within  $1/4V_{FS-2nd}$ ), which is achieved by using a large input differential pair operating in the sub-threshold region.

## IV. CAPACITIVE DAC AND MDAC DESIGNS

Fig. 3 shows the 1<sup>st</sup>-stage SAR architecture with the residue amplification. This design utilized a binary weighted DAC with two sub-capacitive arrays  $DAC_C$  and  $DAC_A$ , each containing 64 units for different functions. During  $\Phi_S$  the input voltage pre-charges the total DAC array. Then, the  $DAC_C$  performs 6b binary-searched conversion, while the  $DAC_A$  keeps connecting to  $V_{cm}$  that serves as the capacitive-dividing by 2 of the supply to match the required reference level. The solution prevents the use of resistive-ladder/buffer for low power consideration, which is similar to that was done in [2][3], while this work achieve more design benefit from the sub-CDAC for the flip-around MDAC implementation.

After the 6b SA conversion, amplification occurs as a flip-around MDAC. The sub-array  $DAC_A$  are separated into  $48C_0$  non-feedback units and the other  $C_{RA}$  of  $16C_0$  that is feedback to op-amp's output for the flip-around amplification by 8. The

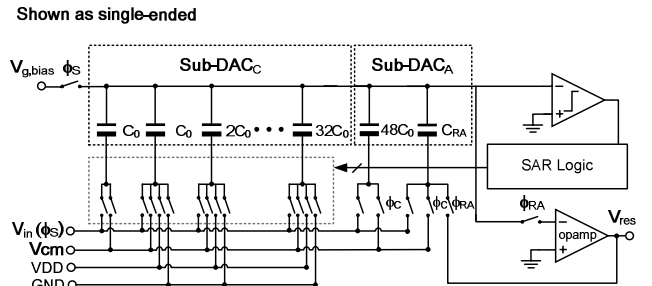


Fig. 3: 1<sup>st</sup>-stage SAR ADC architecture with flip-around MDAC.

residue amplification is solely depends on the ratio of  $\beta=C_{RA}/C_{total}=1/8$ , which is decoupled with the resolution of the complete DAC array. This improved feedback factor in pipelined-SAR ADC.

Since two channels share the same op-amp, the DAC reset is at a reference voltage  $V_{g,bias}$  instead of op-amp's output. The cost is an offset dependence that is, however, the same for the two channels and is kept at its minimum by design. Thus, the op-amp generates the residual of one channel during the even sampling periods and the residual of the other during the odd periods. The value of the unit capacitor ( $5.6\mu\text{m}\times 5.6\mu\text{m}$  equivalent to 13fF) of 1<sup>st</sup>-stage DAC complies with matching requirements. The total sampling capacitance is 1.66pF.

For the 2<sup>nd</sup>-stage DAC design the residue amplification by 8 imposes the reference voltages of 2<sup>nd</sup>-SAR equal to  $\pm 1/8V_{DD}$ . Since the plain split solution of the 1<sup>st</sup>-stage would require a too large capacitance that possibly affects the op-amp's slew-rate and GBW requirements, the capacitive DAC in the second stage employs a capacitive attenuator as shown in Fig. 2. The total capacitance to fulfill the 2<sup>nd</sup>-stage kT/C noise limit is 177fF. The used unit capacitor is ( $5\mu\text{m}\times 5\mu\text{m}$ ) of 10.53fF. The value of the capacitance of  $C_{att}$  ( $8.9\mu\text{m}\times 8.9\mu\text{m}$  equivalent to 31.25fF) is enough to compensate for the gain error caused by the parasitic of internal and external nodes of the DAC array. Accounting for the foreseeable gain mismatch due to process variation, the expected SNDR degradation is just 0.5dB without gain calibration.

## V. CIRCUIT IMPLEMENTATION

Both op-amp and comparator are implemented for low power consideration. The architecture of the op-amp [1] is shown in Fig. 4, which exploits the low output voltage swing by using a telescopic configuration with gain-boost. The control of the current bias enables the tracking of process variations. The used currents keep transistors in the sub-threshold, thus minimizing overheads and making possible a 1.1-V supply. Since the boosting branches must enhance the gain at low frequency they can consume little power, just 7% of the total current burnt by the entire op-amp (700 $\mu$ A). The op-amp achieves a low frequency gain of 67dB gain, 1.36GHz GBW and 73 $^\circ$  phase margin with  $\beta=1/8$ .

Differential dynamic latches without pre-amplifier make the comparators [6] used in this design. Fig.5 shows the schematic of the comparator with NMOS transistors at input. When the strobe is off, there is no current flowing. The relevant nodes are reset to cancel the memory of the previous status. The use of very small

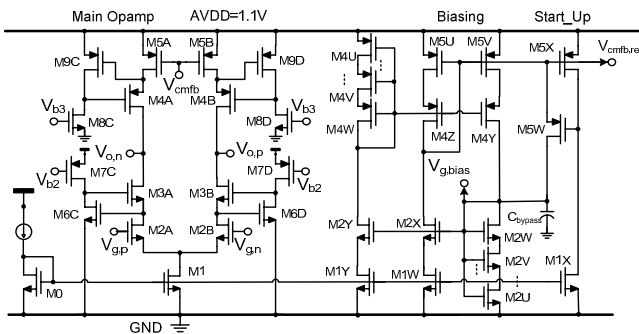


Fig.4: The circuit schematic of the op-amp.

transistors minimizes the parasitic, thus obtaining very high speed even with one LSB imbalance at input. However, a small area of the transistors' gate give rise to large mismatches and, consequently, large input referred offset. Thankfully, the used on-chip offset calibrations compensate for that limit and allow a very low power implementation of the comparators.

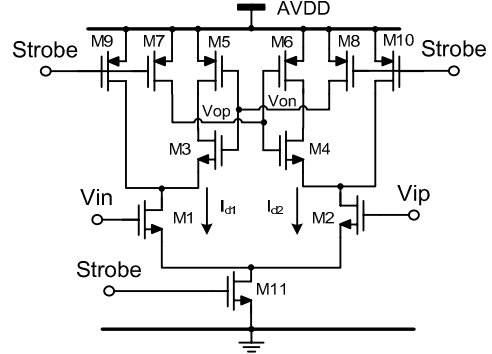


Fig.5: The circuit schematic of 2<sup>nd</sup>-stage dynamic comparator.

## VI. MEASUREMENT RESULTS

The 10-bit TI pipelined-SAR was implemented in 1P7M 65nm CMOS process with metal-oxide-metal (MOM) capacitor. Fig.6 shows the die photograph; the active area is 0.21mm<sup>2</sup>. All the calibrations, including the ones of the 1<sup>st</sup> and 2<sup>nd</sup> stage offsets, are implemented on-chip. Fig.7 shows the measured dynamic performances of the combined two and one of interleaved channels. The ADC achieves a SNDR of 55.4dB at 1.5MHz input frequency and loses 3.2 dB (52.2dB) near the Nyquist frequency (79MHz) with a conversion rate equal to 160 MS/s. The channel mismatches denotes a drop of the SNDR by 0.5dB. Fig.8 shows the measured FFT plotted with 1.5MHz input frequency at 160MS/s sampling rate. Fig.9(a) shows the static performance when calibration is not active. The DNL and the INL without calibration are quite large at the full scale of the 2<sup>nd</sup> SAR that carries a new LSB of 1<sup>st</sup> SAR. The large errors are due to the comparator offsets that cause the 2<sup>nd</sup>-stage to saturate. When calibration is active, as shown in Fig.9(b), the DNL improves from 27.6 LSB to 0.46LSB and the INL from 16.7LSB to 1.7LSB.

Table I summarizes the overall measured performance. The analog power consumption is 1.35mW. The digital power including the SAR logic, offset calibration and clock generator is 1.37mW. The total power consumption is 2.72mW at 160MS/s from 1.1V supply. Table II compares the FoM with state-of-the-art pipelined-SAR ADCs. This work achieves the lowest FoM for the considered high-speed.

## VII. CONCLUSIONS

Self-embedded offset cancellation and the CDACs for two stage SAR ADCs have been presented. The offset cancellation enables a more relaxed calibration range with less additional offset calibration effort, thus allowing the implementation of high-speed and low-power comparators. The design of CDACs allows both flip-around MDAC amplification and prevents the use of reference generator that consumes static power. The ADC

achieves 8.9b ENOB without any gain calibration. The prototype ADC draws only 2.72mW power from the 1.1-V supply and has a FoM of 35fJ/conv.-step.

#### ACKNOWLEDGMENT

The authors would like to thank Hou-Lon Choi (Justin) for the measurement support.

#### REFERENCES

[1] Sai-Weng Sin, et Al., "An 11b 60MS/s 2.1mW Two-Step Time-Interleaved SAR-ADC with Reused S&H," in *ESSCIRC Dig. Tech. Papers*, pp. 218-221, Sep.2010.  
 [2] M. Yoshioka, et Al., "A 10b 50MS/s 820μW SAR ADC with On-Chip Digital Calibration," *ISSCC Dig. Tech. Papers*, pp. 384-385, Feb. 2010.  
 [3] C. C. Lee, M. P. Flynn, "A 12b 50MS/s 3.5mW SAR Assisted 2-Stage Pipeline ADC," in *Symp. VLSI Circuits Dig. Tech. Papers*, pp.239-240, Jun. 2010.

[4] M. Furuta, M. Nozawa, T. Itakura, "A 0.06mm<sup>2</sup> 8.9b ENOB 40MS/s Pipelined SAR ADC in 65nm CMOS," *ISSCC Dig. Tech. Papers*, pp. 382-383, Feb. 2010.  
 [5] Young-DeukJeon, et Al., "A 9.15mW 0.22mm<sup>2</sup> 10b 204MS/s Pipelined SAR ADC in 65nm CMOS" in *CICC Dig. Tech. Papers*, pp. 1-4, Oct. 2010.  
 [6] G. Van der Plas, B. Verbruggen, "A 150MS/s 133μW 7b ADC in 90nm digital CMOS Using a Comparator-Based Asynchronous Binary-Search sub-ADC," *ISSCC Dig. Tech. Papers*, pp. 242-243, 2008.

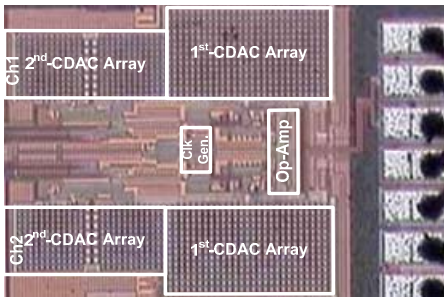


Fig. 6: Die microphotograph of the ADC.

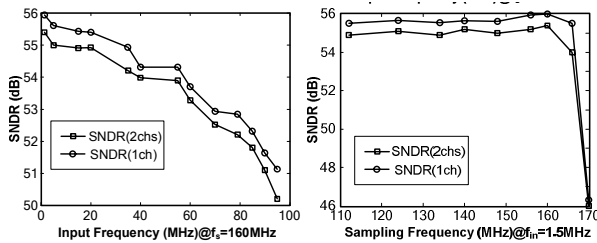


Fig. 7: Measured Dynamic performances.

Table I Summary of performance

Technology	65-nm CMOS
Resolution	10-bit
Sampling Rate	160-MS/s
Supply Voltage	1.1-V
Full Scale Analog Input	1.1-V <sub>pp</sub>
SNDR	55.4dB
SFDR	61.3dB
ENOB	8.9-bit
DNL	+0.46/-0.3LSB
INL	+1.3/-1.7LSB
Power Consumption	
Analog	1.35mW
Digital	1.37mW
Total	2.72mW
FoM	35 fJ/conv.-step

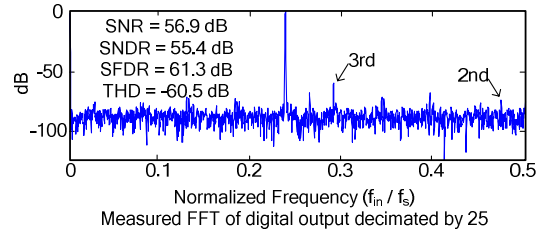


Fig. 8: FFT of the digital output. The input is a 1.5MH sine wave (full-scale) sampled at 160MS/s.

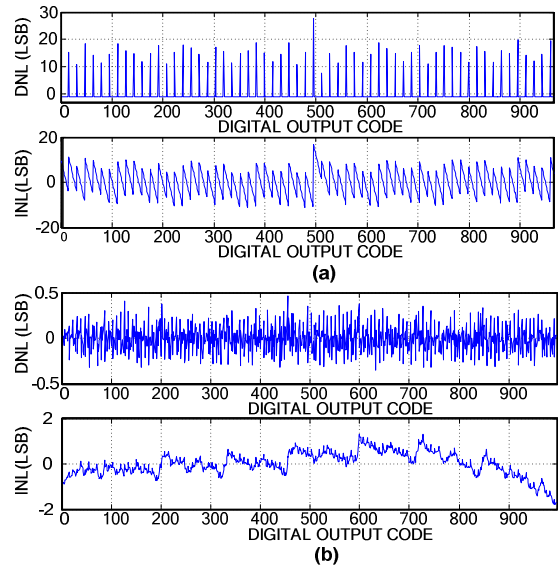


Fig.9: Measured INL and DNL. (a) Without offset calibration. (b) With offset calibration.

Table II Comparison to state-of-the-art works

	[3]	[4]	[5]	This work
Architecture	VLSI' 10 Pipelined-SAR	CICC' 10 Pipelined-SAR	ISSCC' 10 Pipelined-SAR	Pipelined-SAR
Technology (nm)	65	65	65	65
Resolution (bit)	12	10	10	10
Sampling Rate (MS/s)	50	204	40	160
Input Range V <sub>pp</sub> (V)	2	N/A	1	1.1
Supply Voltage (V)	1.3	1	1.1	1.1
SNDR (dB)	66	55.2	55.1	55.4
ENOB (bit)	10.4	8.87	8.86	8.91
Power (mW)	3.5	9.15	1.21	2.72
FoM (fJ/conv.-step)	52	95.4	65	35